3-18-2020

Thin Dry Silicon Oxide Films Grown by Thermal Oxidation

Manisha Muduli

Hiromichi Yamamoto

Thin Dry Silicon Oxide Films Grown by Thermal Oxidation

Abstract

Dry thermal oxidation is performed at 900, 950, 1000, and 1050 C in fused silica tube furnace (Sandvik) for 10, 20, 50, 100 and 200 min. The results are analyzed by both of Deal-Grove model and the method of Gerlach, Maser, and Saad. In the analysis using the Deal-Grove model, the parabolic rate constants are obtained to be 2.1, 7.0, 17.5, and 42.4 nm^2/min at 900, 950, 1000, and 1050 C, respectively, and the linear rate constants are acquired to be 0.2, 0.4, 0.8, and 1.2 nm/min at 900, 950, 1000, 1050 C, respectively. Activation energies of the parabolic rate constant and the linear rate constant are obtained to be 2.67 and 1.55 eV, respectively. In the analysis using the method of Gerlach, Maser, and Saad, the activation energy of the oxide growth rate for the 5 nm thick oxide is obtained to be 2.49 eV, whereas that for the 40 nm thick oxide to be 1.93 eV. The film uniformity for 30 nm thickness shows more than 10%, while that for the thickness of more than 50 nm indicates less than 5%, suggesting that measurement on 30 nm thick film using Filmetrics F50 is not still accurate enough. Standard deviation and coefficient of variation are also examined to discuss the film uniformity.

Keywords

Thermal oxidation, dry oxide, Deal-Grove model, film uniformity

Disciplines

Engineering | Physical Sciences and Mathematics

Thin Dry Silicon Oxide Films Grown by Thermal Oxidation

Manisha Muduli and Hiromichi Yamamoto[1, a)]
[1]*Singh Center for Nanotechnology, University of Pennsylvania*
3205 Walnut St. Philadelphia, PA 19104

(Dated: Received 15 January 2020; accepted 18 March 2020)

Dry thermal oxidation is performed at 900, 950, 1000, and 1050 °C in fused silica tube furnace (Sandvik) for 10, 20, 50, 100 and 200 min. The results are analyzed by both of Deal-Grove model and the method of Gerlach, Maser, and Saad. In the analysis using the Deal-Grove model, the parabolic rate constants are obtained to be 2.1, 7.0, 17.5, and 42.4 nm^2/min at 900, 950, 1000, and 1050 °C, respectively, and the linear rate constants are acquired to be 0.2, 0.4, 0.8, and 1.2 nm/min at 900, 950, 1000, 1050 °C, respectively. Activation energies of the parabolic rate constant and the linear rate constant are obtained to be 2.67 and 1.55 eV, respectively. In the analysis using the method of Gerlach, Maser, and Saad, the activation energy of the oxide growth rate for the 5 nm thick oxide is obtained to be 2.49 eV, whereas that for the 40 nm thick oxide to be 1.93 eV. The film uniformity for ∼30 nm thickness shows more than 10%, while that for the thickness of more than 50 nm indicates less than 5%, suggesting that measurement on 30 nm thick film using Filmetrics F50 is not still accurate enough. Standard deviation and coefficient of variation are also examined to discuss the film uniformity.

Key Words: Thermal oxidation, dry oxide, Deal-Grove model, film uniformity

I. Introduction

SiO_2 thin films are conventionally grown for device applications using standard furnaces with long oxidation times (>20 min) and low partial pressures of oxidant. This process of oxide growth on silicon is widely known as thermal oxidation of silicon. Thermal oxidation of silicon leads to the formation of an interfacial layer of silicon dioxide between the surface silicon dioxide and the silicon substrate (Figure 1). The interfacial layer has been characterized to be ∼1 nm.[1] The thermal oxidation of silicon has been considered to follow the three steps: (1) the oxidizing gas approaches to the sample surface, and reacts and is absorbed at the sample surface. (2) the oxidant molecules transport from the surface of the oxide to the silicon through the oxide, and (3) the oxidation reaction at the interface between the oxide and silicon.[2] Although new theories of thermal oxidation of silicon[3–9] have been reported since Deal-Grove model,[2] it should be pointed out that the basic mechanisms of the early formation stages at SiO_2/Si interface are still an open question.[10]

The goal of this project is to perform on-site inspection of thermal oxidation of silicon to collect the basic data on the fused silica tube furnace (Sandvik) at Quattrone Nanofabrication Facility. The data will be analyzed by Deal-Grove model[2] and the method of Gerlach, Maser, and Saad.[10] In addition, the thickness uniformity will be analyzed by uniformity formula, standard deviation, and coefficient of variation.

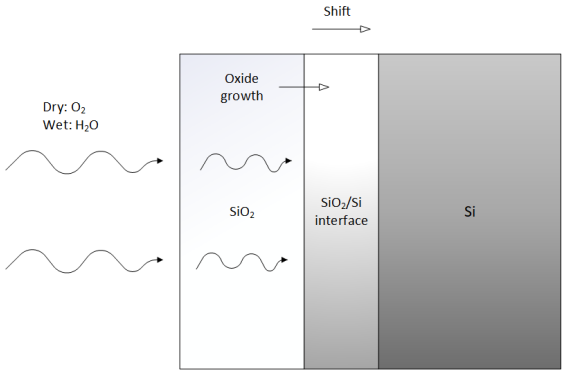

FIG. 1. Thermal oxidation of silicon

II. Experiment

4" diameter single side polished p-type boron doped (100) Si wafers were used for measuring the oxide film thicknesses. The thickness and electrical resistivity of the wafers were 525±25 μm and 1-20 Ω·cm, respectively. These wafers were RCA cleaned prior to the high temperature oxidation of the wafers. Dry thermal oxidation was performed at 900, 950, 1000, and 1050 °C for 10, 20, 50, 100 and 200 min in fused silica tube furnace (Sandvik). The thicknesses of the SiO_2 thin films were measured using a Woollam VAS ellipsometer and a Filmetrics F50 reflectometer. The Cauchy model was used to analyze

[a)]Electronic mail: hyam@seas.upenn.edu

the thickness when using the ellipsometer. The thickness uniformity was measured using the reflectometer.

III. Results and Discussion

A. Oxide Growth and Activation Energy

An oxidation time dependence of the oxide growth on silicon has been given by Deal-Grove model,[2] as follows:

$$x^2 + Ax = B(t + \tau) \tag{1}$$

where x and t are the oxide thickness and oxidation time. A, B, and τ are given by the following equations:

$$A = 2D_{eff}\left(\frac{1}{k} + \frac{1}{h}\right) \tag{2}$$

$$B = \frac{2D_{eff}\,C^*}{N_1} \tag{3}$$

$$\tau = \frac{x_0^2 + Ax_0}{B} \tag{4}$$

where D_{eff} is effective diffusion coefficient in the oxide, k is the rate constant of the first order reaction at the interface between the oxide and silicon, h is the gas-phase transport coefficient of the oxidizing gas from the external surface to the sample surface, C^* is the equilibrium concentration of the oxidant in the oxide, N_1 is the number of oxidant molecules incorporated into a unit volume of the oxide layer, and x_0 is the initial oxide thickness on the Si surface. From Eqs. (2) and (3), B/A is given by the following equation:

$$\frac{B}{A} = \frac{kh}{k+h}\frac{C^*}{N_1} \tag{5}$$

Since h >> k,[2] Eq. (5) can be approximated by the following equation:

$$\frac{B}{A} \cong k\frac{C^*}{N_1} \tag{6}$$

Thus, B/A is proportional to a rate constant of the oxidation reaction at the interface between the oxide and silicon. B and B/A are referred to as the parabolic rate constant and the linear rate constant, respectively. Eq. (1) can be rewritten as

$$x = \frac{B(t+\tau)}{x} - A \tag{7}$$

From Eq. (7), a plot of x vs t/x gives -A from an intercept at $t/x = 0$ when $\tau = 0$, and B from the slope of the plot. Table I indicates the dry oxide thicknesses processed for 10, 20, 50, 100 and 200 min at 900, 950, 1000, and 1050 °C. Figure 2 shows a plot of x vs t/x,

TABLE I. The dry oxide thicknesses processed for 10, 20, 50, 100 and 200 min at 900, 950, 1000, and 1050 °C. The data includes the native oxide thickness of ~1.3 nm.

Time(min)	Oxide Thickness (nm)			
	900 °C	950 °C	1000 °C	1050 °C
10	3.4	5.0	7.7	11.7
20	4.6	7.0	11.5	18.0
50	7.4	12.4	20.8	32.0
100	11.4	19.9	33.4	51.0
200	18.2	31.8	50.4	79.2

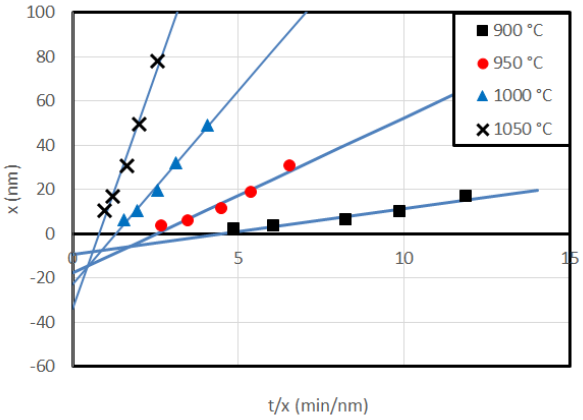

FIG. 2. A plot of x vs t/x. The black squares, red circles, blue triangles, and crosses show the measured thicknesses processed at 900, 950, 1000, and 1050 °C, respectively. The solid blue lines are the linear trend lines. The native oxide thickness of 1.3 nm is subtracted from the measured thicknesses. The intercept at $t/x = 0$ indicates -A, and the slope gives B in Eq. (7).

TABLE II. The values of A, B, and B/A obtained from the intercepts at $t/x = 0$ and the slopes in Figure 2 at 900, 950, 1000, and 1050 °C.

	900 °C	950 °C	1000 °C	1050 °C
A (nm)	9.2	17.8	23.0	34.0
B (nm^2/min)	2.1	7.0	17.5	42.4
B/A (nm/min)	0.2	0.4	0.8	1.2

where the native oxide thickness of 1.3 nm is subtracted from the measured thicknesses. Table II indicates the values of A and B obtained from the intercepts at $t/x = 0$ and the slopes at 900, 950, 1000, and 1050 °C in Figure 2. B/A listed in Table II is discussed later.

An oxidation time dependence of the oxide growth is discussed using the values of A and B obtained above. Eq. (1) can also be rewritten as

$$\left(x + \frac{A}{4}\right)^2 = B(t+\tau) + \frac{A^2}{4} = \frac{A^2 + 4B(t+\tau)}{4} \tag{8}$$

From Eq. (8), the oxidation time dependence of the

oxide growth is given by the following equation:

$$x = \frac{-A + \sqrt{A^2 + 4B(t+\tau)}}{2} \tag{9}$$

Figure 3 shows the measured oxide thicknesses processed at 900, 950, 1000, and 1050 °C for 10, 20, 50, 100, and 200 min. Figure 3 also depicts the thicknesses calculated by Eq. (9) using the parameters A and B in Table II. The native oxide thickness of 1.3 nm is subtracted from the measured oxide thicknesses. As can be seen in Figure 3, the measured and calculated thicknesses are in good agreement.

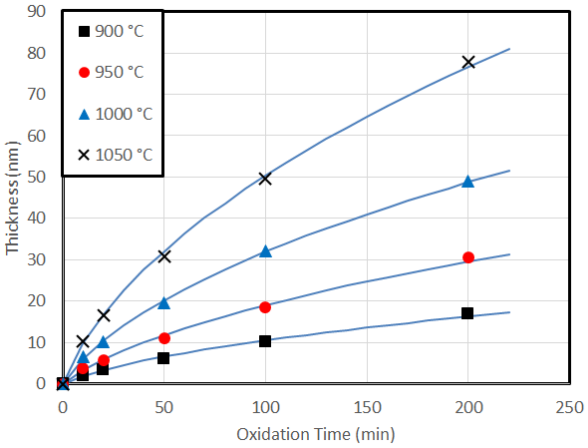

FIG. 3. An oxidation time dependence of the dry oxide thickness. The black squares, red circles, blue triangles, and crosses show the measured thicknesses processed at 900, 950, 1000, and 1050 °C, respectively. The blue solid curves are the thicknesses calculated by Eq. (9) and the parameters A and B in Table II. The native oxide thickness of 1.3 nm is subtracted from the measured thicknesses.

Figure 4 shows Arrhenius plots of B and B/A against $1000/T$, from the slopes of which activation energies are obtained to be 2.67 and 1.55 eV, respectively. On the other hand, the activation energy of B has been reported to be from 1.2 to 1.4 eV,[2,11,12] while the activation energy of B/A has been shown to be from 0.2 (theorical) to 2.0 (experimental) eV.[10] The result of the present study is clearly in poor agreement with the results reported previously. The cause of the disagreement is unknown.

As described above, Deal-Grove model has been criticized that it cannot describe the kinetics of the oxidation process in principle. G. Gerlach *et al.*[10]obtained activation energy by analyzing data on the oxide thickness and the oxidation time without any physical model. It is pointed out that the oxide growth rate R can be expressed by Arrhenius relation:[10,13]

$$R = R_0 \exp\left(-\frac{E_A}{k_B T}\right) \tag{10}$$

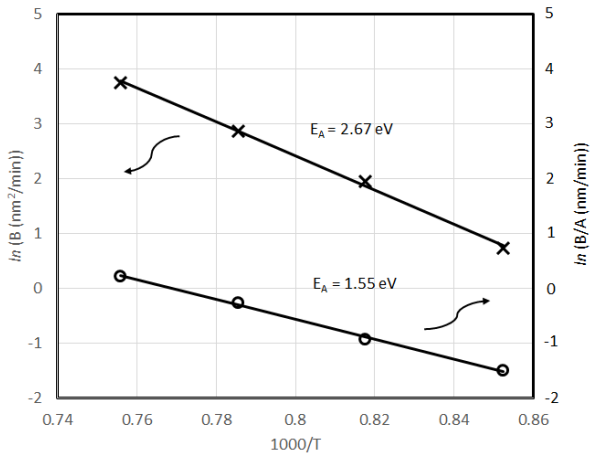

FIG. 4. Arrhenius plots of the parabolic rate constant B and the linear rate constant B/A.

where R is the oxide growth rate, R_0 is the preexponential factor of R, E_A is the activation energy, k_B is Boltzmann constant, and T is the absolute temperature. From eq. (10), the activation energy E_A is given by the following equation:

$$E_A = k_B \frac{\ln(R_2) - \ln(R_1)}{1/T_1 - 1/T_2} \tag{11}$$

where R_i is the oxide growth rate of the i-th interval of the oxide thickness and oxidation time at T_i. The oxide thickness and time during the i-th interval is taken an average by the following equations:

$$L_{m_i} = \frac{L_i + L_{i+1}}{2} \tag{12}$$

$$t_{m_i} = \frac{t_i + t_{i+1}}{2} \tag{13}$$

where m means the mean value of the i-th interval. The differential between the i-th and $(i+1)$-th intervals of the oxide thickness and oxidation time can be calculated by the following equations:

$$\Delta L_{m_i} = L_{i+1} - L_i \tag{14}$$

$$\Delta t_{m_i} = t_{i+1} - t_i \tag{15}$$

The oxide growth rate is given by the following equation:

$$R_{m_i} = \frac{\Delta L_{m_i}}{\Delta t_{m_i}} \tag{16}$$

Figure 5 shows a plot of natural logarithm of the oxide growth rate versus the mean oxide thickness. The broken lines represent logarithmic trend lines. Table III indicates activation energies at the mean oxide thickness at each temperature, which are obtained by eq. (11) and reading of the logarithmic tend lines. As shown in Table III, activation energy for 5 nm thick oxide is obtained to be 2.49 eV, while that for 40 nm thick oxide to be 1.93 eV. In other words, the activation energy for the oxide growth rate decreases with increase in the distance from the Si substrate. This tendency has also been reported by G. Gerlach *et al.*[10] Their activation energies were from 2.1 to 1.9 eV for the oxides of 5 to 30 nm thickness in the temperature range between 780 and 930 °C. In this study, activation energies between 900 and 950 °C are shown to be ∼2.5 eV, while those between 1000 and 1050 °C to be 1.9 to 2.1 eV.

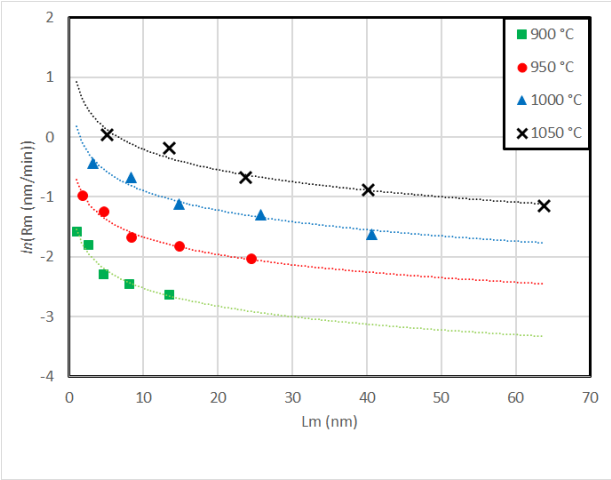

FIG. 5. A plot of natural logarithm of the oxide growth rate versus the mean oxide thickness. Logarithmic trend lines are shown by the broken lines.

TABLE III. Activation energies for the mean oxide thickness using Eq. (11) and the reading of the logarithmic trend lines. (Note) Activation energies at 20 to 40 nm at T_1 = 900 °C and at 30 to 40 nm at T_1 =950 °C are not obtained due to no experimental data.

T_2	950 °C	1000 °C	1050 °C	1000 °C	1050 °C	1050 °C
T_1	900 °C	900 °C	900 °C	950 °C	950 °C	1000 °C
Lm (nm)	Activation energy (eV)					
5	2.45	2.13	2.11	2.17	2.12	2.06
10	2.48	2.09	2.07	2.08	2.05	2.02
15	2.49	2.08	2.05	2.02	2.01	1.99
20	···	···	···	1.99	1.98	1.97
25	···	···	···	1.96	1.96	1.96
30	···	···	···	···	···	1.95
40	···	···	···	···	···	1.93

TABLE IV. Comparison of the oxide film thicknesses measured by Filmetrics F50 with those measured by Woollam Ellipsometer.

	900 °C	950 °C	1000 °C	1050 °C
Oxidation time (min)	Film thickness (nm)			
	Filmetrics F50 Mean film thickness of 85 points			
10	0.2	0.4	0.7	7.1
20	0.2	1.7	6.4	16.3
50	0.4	6.8	18.4	31.3
100	3.6	16.5	33.6	51.5
200	14.2	30.7	50.7	79.2
	Woollam Ellipsometer Film thickness of single point			
10	3.4	5.0	7.7	11.7
20	4.6	7.0	11.5	18.0
50	7.4	12.4	20.8	32.0
100	11.4	19.9	33.4	51.0
200	18.2	31.8	50.4	79.2

B. Film uniformity

Since the film uniformity is discussed by the thicknesses measured by a Filmetrics F50 reflectometer, reliability in the thin film thickness is examined with the result of a Woollam VAS ellipsometer, which is very precise even in the range of 1 nm. Table IV indicates comparison of the oxide film thicknesses measured by a Filmetrics F50 with those measured by a Woollam ellipsometer. As can be seen in Table IV, the thicknesses of more than 30 nm measured by Filmetrics F50 are in good agreement with those by Woollam ellipsometer, although the specification of Filmetrics F50 indicates the thickness range of 20 nm to 70 μm. Hereafter, the film uniformity will be discussed using the thicknesses of more than 30 nm, due to the above reason.

Film thickness uniformity is generally calculated by the following equation:

$$\text{Film uniformity } (\%) = \frac{\max - \min}{\max + \min} \times 100 \qquad (17)$$

or

$$\text{Film uniformity } (\%) = \frac{\max - \min}{\text{average}} \times 100 \qquad (18)$$

A large value number of film thickness uniformity means that the difference between the maximum and minimum thickness is large, according to eq. (17) or (18), so that the film thickness uniformity is poor. It is also referred to as non-uniformity. In other words, film thickness uniformity is determined by the maximum and minimum values. On the other hand, standard deviation shows how spreading out the thickness population is, and is given by the following well-known equation:

$$\sigma = \sqrt{\frac{\sum (x_i - \mu)^2}{N}} \qquad (19)$$

TABLE V. Uniformity, standard deviation, and coefficient of variation of the film thicknesses of more than 30 nm.

Oxidation time (min)	950 °C	1000 °C	1050 °C
Uniformity (%)			
50	···	···	10.9
100	···	29.6	4.6
200	15.5	4.2	2.2
Standard deviation (nm)			
50	···	···	1.2
100	···	2.0	1.0
200	1.6	0.9	0.9
Coefficient of Variation			
50	···	···	0.038
100	···	0.060	0.019
200	0.053	0.018	0.011

where σ is standard deviation of the thickness population, N is the size of the thickness population (or the number of the data points), x_i is each thickness of the data point, and μ is the thickness mean. Another measure of uniformity is "coefficient of variation", which is calculated by the following equation:

$$\text{Coefficient of variation} = \frac{\sigma}{\mu} \tag{20}$$

Coefficient of variation of the thickness manifests how much the thickness of the film on the entire substrate is varying with respect to the average thickness of film. Table V indicates uniformity, standard deviation, and coefficient of variation of the film thicknesses of more than 30 nm. As indicated in Table V, the uniformity for the thickness of ∼30 nm is more than 10 %, while that for the thickness of more than 50 nm is less than 5 %, meaning that the uniformity for the thickness of ∼30 nm is twice worse than that for the thickness of more than 50 nm. Standard deviation for the thickness of ∼30 nm shows to be 1.2 to 2.0 nm, whereas that for more than 50 nm is 0.9 to 1.0 nm. Coefficient of variation for the thickness of ∼30 nm displays to be 0.038 to 0.060, while that for the thickness of more than 50 nm indicates to be 0.011 to 0.019. This result implies that Filmetrics F50 around 30 nm is not still accurate enough. In addition, coefficient of variation is shown to be a good measure of the film uniformity.

IV. Summary

Dry thermal oxidation was performed at 900, 950, 1000, and 1050 °C in fused silica tube furnace (Sandvik) for 10, 20, 50, 100 and 200 min. The result was analyzed using both of Deal-Grove model and the method of Gerlach, Maser, and Saad. In the Deal-Grove analysis, the parabolic rate constants B were obtained to be 2.1, 7.0, 17.5, and 42.4 nm^2/min at 900, 950, 1000, and 1050 °C, respectively, and the linear rate constants B/A were acquired to be 0.2, 0.4, 0.8, and 1.2 nm/min at 900, 950, 1000, 1050 °C, respectively. Activation energies of B and B/A were obtained to be 2.67 and 1.55 eV, respectively. In the analysis by the method of Gerlach, Maser, and Saad, the activation energy for the oxide growth rate decreases from 2.49 to 1.93 eV with increase in the distance from 5 to 40 nm from the Si interface. The film uniformity for ∼30 nm thickness was obtained to be more than 10 %, while that for the thickness of more than 50 nm is less than 5 %, suggesting that Filmetrics F50 is not still accurate enough. Standard deviation and coefficient of variation were also examined to discuss the film uniformity. As a result, it turns out that coefficient of variation is a good measure of the film uniformity.

V. Acknowledgements

This work was performed at the Singh Center for Nanotechnology at the University of Pennsylvania, a member of the National Nanotechnology Coordinated Infrastructure (NNCI) network, which is supported by the National Science Foundation (Grant NNCI-1542153).

[1] Y. Song P. Li and X. Zuo. *Physics Status Solidi Rapid Research Letters*, 13, 2019.
[2] B. E. Deal and A. S. Grove. *Journal of Applied Physics*, 36, 1965.
[3] N. Mousseau N. Salles, N. Richard and A. Hemeryck. *Journal of Chemical Physics*, 147, 054701, 2017.
[4] A. Bongiorno and A. Pasquarello. *Physics Review Papers*, 88, 2002.
[5] A. Bongiorno and A. Pasquarello. *Physics Review Papers*, 83, 2002.
[6] A. Bongiorno and A. Pasquarello. *Physics Review B*, 70, 2004.
[7] L. Tsetseris and S. T. Pantelides. *Physics Review Letters*, 97, 2006.
[8] G. Gerlach and K. Maser. *Advanced Condensed Matter Physics*, 2016.
[9] K. Tatsumura T. Watanabe and I. Ohdomari. *Physics Review Letters*, 96, 2006.
[10] K. Maser G. Gerlach and A. M. Saad. *Physics Status Solidi B*, 246, 2009.
[11] F. J. Norton. *Nature*, 191, 1961.
[12] R. R. Razouk L. N. Lie and B. E. Deal. *Journal of Electrochemical Society*, 129, 1982.
[13] K. Maser. *Journal of Solid State Electrochemistry*, 23, 2019.